ARCNL ADVANCED RESEARCH CENTER FOR NANOLITHOGRAPHY — UNIVERSITY OF AMSTERDAM — VU VRIJE UNIVERSITEIT AMSTERDAM

# Comparing the simulation thickness profile and expansion curve to those of experiments

Tom Bierens, 14565587

Date of submission: July 9, 2025
Conducted between: March 26th, 2025 - July 9th, 2025

| | | | |
|---|---|---|---|
| Study | Physics and Astronomy | Responsible supervisor | Oscar Versolato |
| Research institute | ARCNL | Daily supervisor | Hugo Franca |
| Studentnumber | 14565587 | Examinator | John Sheil |

# 1 Abstract

In this research, we simulate a tin droplet being hit by a laser using the Basilisk flow solver. When the droplet is hit, it flattens into a sheet with a rim that expands and later retracts. During this process, ligaments can be shed from the rim, and we are interested in predicting how this happens by analyzing the thickness profile of the sheet and the expansion curve.

We run nine simulations using three different Weber numbers ($We = 100, 200, 500$) and three different values for the width of the pressure profile, which is a raised cosine with $W$ indicating the width ($W = 1.5, 1.75, 2$). From each simulation, we extract the sheet thickness and its radius over time. We use non-dimensional values and use the models in this paper to collapse the curves to show a clear pattern in how the sheet evolves. We also extract the expansion curves and compare them with models and experiments from literature.

We find that the sheet expands later in the simulations than in experiments. This is likely due to the lack of mass shedding in the simulated rim, which would otherwise lower the rim mass and causes it to retract earlier. Lastly, we test an identity that links the expansion and thickness profile models and find that our simulation parameters do not match the identity, because of the lack of mass shedding.

# Contents

## 2 Introduction and context

Droplets and their dynamics are important in multiple industries, for example, combustion engines, where fuel and air mix in a carburetor. Here tiny droplets of fuel mix with the air [1]. Another important application of droplets appears in the field of nano-lithography, where the laser-induced deformation of a droplet is used in the process of generating extreme ultraviolet light (EUV). Tin is used because it produces the desired light of 13.5 nm, which lays in the EUV spectrum range that is necessary for nano-lithography. This process happens in two stages, a pre-pulse laser that thins the tin droplet into a sheet and a main pulse that ablates the tin producing EUV light from the resulting plasma. The process that leads the droplet into a sheet has a complex mass distribution, where the droplet evolves into a sheet with a rim. The rim can destabilize, leading to ligaments that protrude and cause debris to shed from the sheet. This process occurs throughout the expansion and retraction of the sheet.

By using the thickness profile of the tin sheet and the expansion curve we can ultimately predict the amount of ligaments that got shed from the sheet during the expansion and retraction phase. By predicting this we can tune the laser and the machine to improve the efficiency of the plasma creation in terms of mass and debris generation.

### 2.1 Research Aims

In this research, we compare the results of an experimental research done by M. Kharbedia et al. [2] and the research of Y. Wang & L. Bourouiba [3], to nine simulations where we vary three different Weber numbers. The Weber number is a number that shows the inertia to the surface tension, and three pressure profiles on the sheet. The pressure profile is a simulation of the pressure being applied by the plasma that formed after the laser impacted on the sheet. In [2] and in [3], the authors found an identity that linked the thickness profile to the expansion curve, to predict the evolution of the tin sheet that got hit by a laser. In experiments, it is extremely hard to measure the thickness profile because it cannot be extrapolated by pictures. This is why we compare the simulations to the experiments. The three Weber numbers used in this research are; $We = 100, We = 200$ and $We = 500$, for each of these numbers we varied the width of the pressure profile, the raised cosine, $W$, we used $W = 1.5, W = 1.75$ and $W = 2$. We chose these numbers because $We$ gives us a range of Weber numbers that are also used in the paper of Y. Wang & L. Bourouiba [3] and higher Weber numbers result in early non-physical sheet breakups. The W-parameter is not changed in these papers, we choose the values of $W$ to be close to the real pressure profile exerted by the laser on the droplet in the nano-lithogrophy machine [4]. So in our research, we want to compare the simulation thickness profiles and expansion curves to those of experiments and does the identity predict the thickness profile from the expansion curve?

# 3 Theory and Method

## 3.1 Navier-Stokes equation

This research uses hydrodynamics to calculate the properties of the tin droplet over time after it is deformed by a laser-induced action in which the droplet forms into a sheet. The equations are governed by the isothermal incompressible bi-phase (droplet and surrounding fluid) flow, which are the continuity and momentum conservation, given by

$$\rho\left(\frac{\partial \vec{u}}{\partial t} + \nabla\cdot(\vec{u}\vec{u})\right) = -\nabla p + \mu\nabla^2\vec{u} + \vec{f}_\gamma, \tag{1}$$

$$\nabla\cdot\vec{u} = 0, \tag{2}$$

where $\vec{u}$ and $p$ are the velocity and pressure fields, respectively. Furthermore, $\rho$ and $\mu$ are the density of the fluid and the viscosity of the fluid [4]. The surface tension force, $\vec{f}_\gamma$, is defined as a body force, which is a force that acts only on the interface of the fluid. The surface tension force is given by $\vec{f}_\gamma = \gamma\kappa\delta_s\vec{n}$, where $\gamma$ is the constant surface tension, $\kappa$ is the local curvature of the interface, $\delta_s$ is the Dirac delta function centered on the interface and $\vec{n}$ is the normal vector on the interface [4].

Equation (1) and equation (2) can be non-dimensionalized by rewriting the variables as follows:

$$\vec{x} = R_0\bar{\vec{x}}, \quad t = \frac{R_0}{U_z}\bar{t}, \quad \vec{u} = U_z\bar{\vec{u}}, \quad p = \rho U_z^2\bar{p}, \quad \kappa = \frac{1}{R_0}\bar{\kappa}, \quad \delta_s = \frac{1}{R_0}\bar{\delta}_s, \tag{3}$$

where $R_o$ is the initial radius of the tin droplet and $U_z$ is the droplet center of mass translation velocity obtained after the laser hits. In this paper, we write the non-dimensional variable with a bar on top. Putting equation (3) into equations (1) and (2) we obtain the following equation:

$$\frac{\partial\bar{\vec{u}}}{\partial t} + \nabla\cdot(\bar{\vec{u}}\bar{\vec{u}}) = -\nabla\bar{p} + \frac{1}{Re}\nabla^2\bar{\vec{u}} + \frac{1}{We}\bar{\kappa}\bar{\delta}_s\vec{n}, \tag{4}$$

where $Re$ is the Reynolds number and $We$ is the Weber number, which are given by the following equations:

$$Re = \frac{\rho U_z R_0}{\mu}, \quad \text{and} \quad We = \frac{\rho U_z^2 R_0}{\gamma}. \tag{5}$$

The Reynolds number gives us the competition between the inertia and the viscosity of the fluid. The Weber number gives us the relation between the inertia and the surface tension of the fluid. Later in the text, we use a different type of Weber number, the deformation Weber number which is given by

$$We_{def} = \frac{2\rho \dot{R}_0^2 R_0}{\gamma}, \tag{6}$$

where $\dot{R}_0$ is the initial expansion velocity of the droplet. The deformation Weber number is used because it captures the expansion mechanics of the laser impulse-induced tin sheet.

### 3.2 Raised cosine pressure profile

To solve equation (4), a pressure profile is needed, representing the initial pressure exerted by the plasma on the surface of the tin droplet. In this work, this profile will be represented by a raised cosine function, as proposed by H. Franca et al [4]. The pressure profile presents the initial condition of the pressure that the plasma exerts on the tin droplet after it is hit by the laser. The raised cosine profile is given as follows:

$$f(\theta) = \frac{1}{2}(1 + \cos(\theta \frac{\pi}{W}))H(W - \theta), \tag{7}$$

$H$ is the standard Heaviside step function, $W$ is the parameter that gives us the width of the pressure profile [4]. The effect of this parameter on the tin droplet will be studied later in our research.

### 3.3 Basilisk

In this research, the simulations are performed by the code named Basilisk. Basilisk is an open source numerical solver based on the coding language C. It solves the Navier-Stokes equations, as shown in equation (4) [5, 6]. By dividing the space into a grid of cells, the discrete equations can be solved for each discrete timestep. This grid consists of cells where the properties are calculated inside and on the boundary of these cells. The calculations are done in fractional steps, which separates the velocity and pressure calculations. Basilisk has a feature called AMR or adaptive mesh refinement, this feature enables the software to refine or improve the amount of cells in complex areas, for example the interface between two liquids [6]. If the mesh or grid has too few points in a certain area the calculations could result in a non-physical break up of the sheet. The experiments are carried out in vacuum. However, in Basilisk we utilize ratios of the viscosity and the density of the two liquids, instead of using a vacuum. The output of basilisk is a VTK-file, this file can store all relevant flow fields within the droplet, such as velocity or pressure, as well as the droplet shape. This output can be visualized by Paraview as seen in figure 1 or post-processed to extract the radius and the thickness of the sheet. These files are an output after every VTK-timestep, $T$ of 0.01.

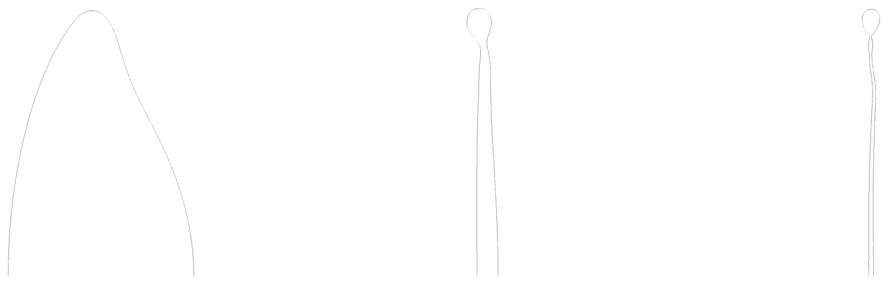

(a) (b) (c)

Figure 1: Droplet interface at three different time instants during its evolution into a sheet. Panel a) shortly after laser-hit, $T = 0.62$, panel b) midway through expansion, $T = 2.62$, and panel c) the sheet late in the expansion phase, $T = 5.55$. This simulation used $We = 200, W = 2$.

## 3.4 Method

### 3.4.1 Extraction and fitting of the thickness profile

The VTK-file also contains polygon points of the interface of the droplet, and these polygon points can be used in Python to make a plot of the droplet. The data from the VTK-file are non-dimensional as given in equation (3). Each Vtk-file corresponds to a timestep of the simulation. For each timestep, we slice the sheet with horizontal lines to get a thickness of the sheet. We also store the radius of the sheet which is defined as the y-axis of the polygon points. If we plot the thickness to the radius we get a thickness profile as seen in figure 2

We multiply the thickness of the sheet by $T^2$, where $T$ is the non-dimensional time. This is done to collapse the y-axis. The radius is divided by $T$ to collapse the x axis, as seen in figure 3. We can then follow the evolution of the thickness profile over time as seen in figure 3. At early times the curve gets stretched out and at later time the curve gets shortened. This is also seen in the rim, which is the bulge in the curve. We see that there is an overlap between the different thickness profiles. We are interested in these points to get a fit for the thickness profile. The fit to the thickness profile will be used later on to predict the evolution of the tin sheet over time, with an identity. We fit using the following model [2, 3]:

$$H = \frac{F}{T^2}, \tag{8}$$

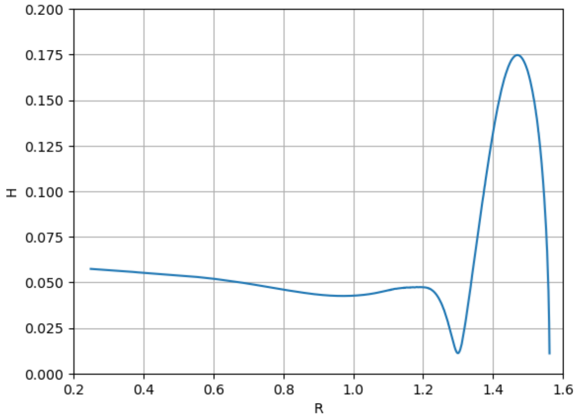


Figure 2: The non-dimensional thickness, $H$, is plotted against the non-dimensional radius, $R$. The blue curve is a thickness profile from $We = 100, W = 2$ at $T = 4.0$.

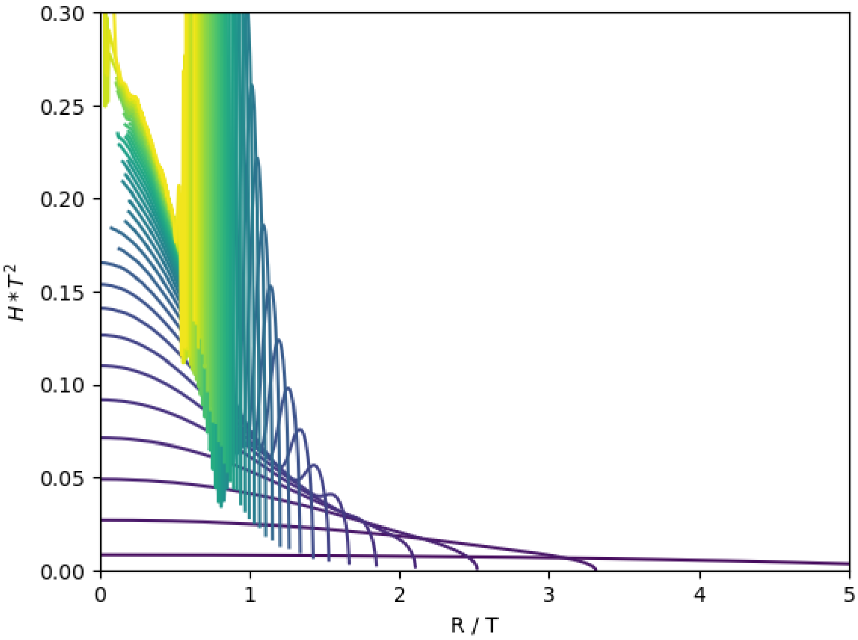


Figure 3: The collapsed non-dimension width, $HT^2$, is plotted against $R/T$. The color of the curves indicate a increase in time, with the darker colors being early time and the bright colors being late time. Each step has $T = 0.2$ between them. We can see a overlap between the curves.

where H is the thickness of the sheet, T is the non-dimensional time and F is

$$F(x) = \frac{1}{a_1 x + a_2 x^2 + a_3 x^3}, \tag{9}$$

x is in this case $R/T$, where R is the non-dimensional radius of the sheet and $a_1$,$a_2$ and $a_3$ are the fit-parameters. We choose the y-axis to be $HT^2$ and the x-axis to be $R/T$. We then get the graph in figure 3. We see that the initial droplet is stretched into a straight long line almost at $HT^2 = 0$ when the time is increased, we observe that the starting point of the thickness profile moves higher up on the $HT^2$-axis and that profile ends at a lower $R/T$. We also note that when we get to later times the bottom of the sheet start to break up because of mesh refinement as seen in figure 4,

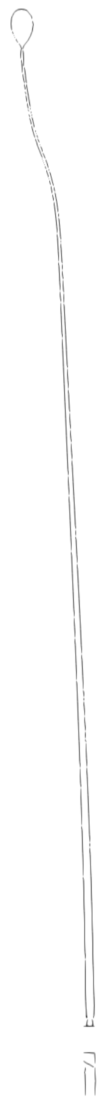

Figure 4: This is a plot of the sheet at $T = 4.8$ from the simulation with $We = 500, W = 1.75$. We see a mesh refinement error at the lower part of the sheet, this results in a non continuous sheet.

so we remove these time steps from the dataset. To obtain a good fit, we use an algorithm to remove the rim of the sheet, since the rim is not included in the models of Y. Wang & L. Bourouiba and M. Kharbedia [3] [2]. The end result is shown in figure 5. After the rim is removed we choose the last 50 points of the thickness profile, this gives us the data points to fit to. In subsection 4.1 we provide the results of the fit.

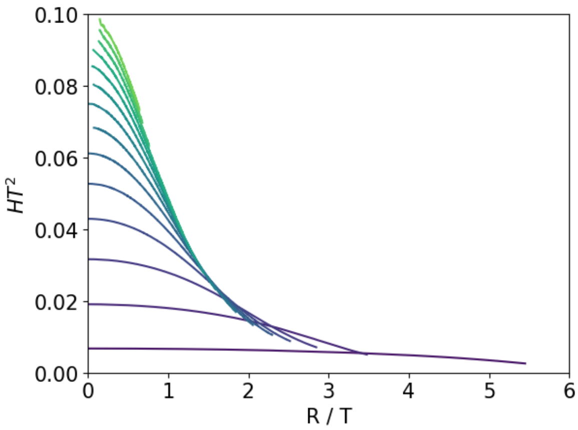


Figure 5: We plotted $HT^2$ against $R/T$. We removed the rim of the thickness profiles. The profiles are plotted with an interval of $T = 0.2$. The darker colors indicate early time and the bright colors indicate later time.

### 3.4.2 Expansion curve

We can also get an expansion curve out of the data as seen in figure 6a. The y-axis is the radius of the sheet, and the time is the non-dimensionalized. By changing the y-axis and the x-axis to $R/R_0\sqrt{We_d}$ and $T/t_c$ respectively, as seen in figure 6b. We change the axes to these values to establish a curve where we can fit to $b_0, b_2, b_3$. We also see in figure 6 where the change in axes results in a collapse of the expansion curves. Where $R/R_0$ is the radius we get from basilisk, $We_d$ is the deformation weber number and $T/t_c$ is the non-dimensional time using the capillary time defined by $t_c = \sqrt{\rho 8R_o^3/6\gamma}$. The deformation Weber number is a number that captures the expansion dynamics of a laser-induced impact that is defined by equation (6) [2] [3]. We can use the following model:

$$\frac{R}{R_0} = \sqrt{We_d}\left(b_3(T-T_m)^3 + b_2(T-T_m)^2 + b_0\right), \tag{10}$$

where $T = t/t_c$, $T_m$ is the non-dimensional time where the expansion curve has an apex, and $b_3, b_2$ and $b_0$ are the fit parameters. Where $b_0$ is the non-dimensional maximum sheet radius scaled as $b_0 = R_{max}/(R_0\sqrt{We_d})$. The physical meaning of $2b_2$ is the deceleration of the rim velocity along the sheet expansion and $b_3$ is related to the initial velocity of the expansion [2].

### 3.4.3 Identity

These two sets of parameters in model (8) and model (10) can be linked via an identity, in this research we use a non-Galilean Taylor-Culick law [3], which is as follows:

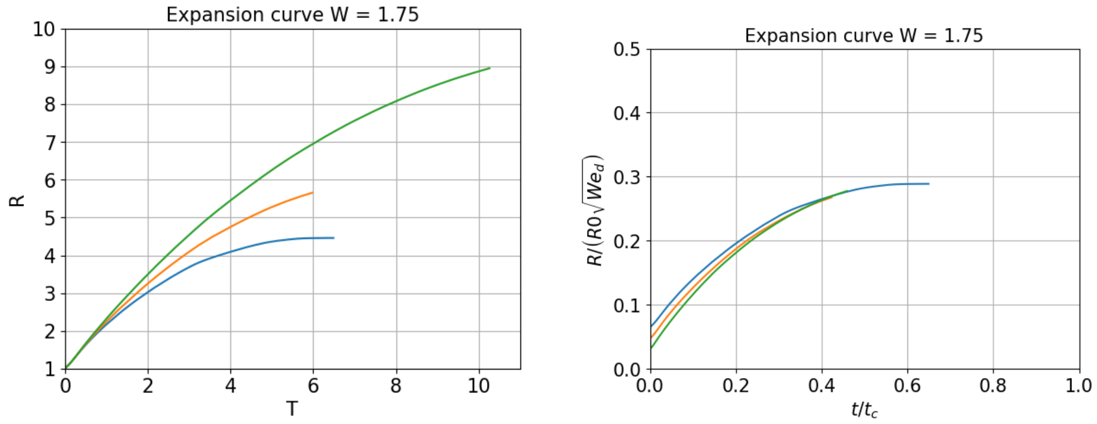


(a) (b)

Figure 6: In figure 6a the non-dimensional radius is plotted against the non-dimensional time. The blue curve is $We = 100, W = 1.75$, the orange curve is $We = 200, W = 1.75$ and the green curve $We = 500, W = 1.75$. In figure 6b is the non-dimensional radius scaled by the $\sqrt{We_d}$ plotted against the scaled non-dimensional time by $t_c$. The expansion curve colors correspond with the ones in figure 6a.

$$-6H(\bar{R},T)\left(\frac{\bar{R}(T)}{T}-\dot{\bar{R}}(T)\right)^2+\left(2-\frac{\pi}{7}\right)=0 \tag{11}$$

where $H(r,T)$, $r(T)$, $\dot{r}(T)$ are the non-dimensionalized sheet thickness, radius, and velocity respectively. This function uses the non-dimensional time $T = t/t_c$. By doing some algebra and a change of variables with,

$$Y = r\sqrt{\frac{6}{We_d}}, \quad U = T - T_m, \tag{12}$$

as can be seen in the paper of M. Kharbedia et al. [2] and the paper of Y. Wang & L. Bourouiba [3]). We obtain,

$$6\left(Y-\dot{Y}(U+T_m)\right)^2=\left(2-\frac{\pi}{7}\right)\left[a_3Y^3(U+T_m)+a_2Y^2(U+T_m)^2+a_1(U+T_m)^3+a_0(U+T_m)^4\right], \tag{13}$$

we can then rewrite it as,

$$Y(U) = \beta_0 + \beta_2 U^2 + \beta_3 U^3, \tag{14}$$

Note that we can now relate the coefficients $b_0$, $b_2$ and $b_3$ with $\beta_0$, $\beta_2$ and $\beta_3$ as follows:

$$(\beta_0, \beta_2, \beta_3) = \sqrt{6}(b_0, b_2, b_3), \tag{15}$$

After putting equation 14 into 13 and with some algebra using mathematica we can obtain and derive $b_0, b_2$ and $b_3$ from $a_1$,$a_2$ and $a_3$. These results can be seen in section 4.3

# 4 Results + Discussion

## 4.1 Thickness profile

We simulated nine different situations in which a tin droplet was hit by a laser. We used three different Weber numbers $We = 100, 200$ and 500, we choose these Weber numbers because higher numbers result in early non-physical break up of the sheet. For each of the Weber numbers we use three different $W$ parameters 1.5, 1.75 and 2. Here, $W$ gives us the width of the pressure profile of the plasma created by the laser [4]. After the laser hits the droplet the droplet flattens, becomes thinner, and stretches. We extract the radius of the droplet and the thickness or width of the droplet. These values are then divided by the radius of the initial droplet. This results in a non-dimensionalized value. In figures 7, 8, 9, 10 is the width times the non-dimensionalized time squared plotted against $R/T$. The orange data are obtained from the simulations mentioned earlier. The earlier times have a higher $R/T$ and a lower $HT^2$, so then from right to left the time increases. The black line is a fit through the orange data points. The pink and blue lines are the parameters $a_1 = 24.4, a_2 = -28.1, a_3 = 35.2$, found by Y. Wang & L. Bourouiba [3], these parameters represent a water droplet falling onto a pillar, and $a_1 = 31.4, a_2 = -30.0, a_3 = 24.4$, found by M. Kharbedia [2] respectively. We note that the fit of $W = 1.5$ matches the models at low $R/T$, so at late times, this can be explained by the laser pressure profile on the sheet is most similar to the raised cosine profile at $W = 1.5$. We observe that the data and the fit moves from left to right in comparison to the $R/T$ - axis with an increase in $W$. This can be seen in figure 7, 8, 9. The increase in $W$ results in a wider impact on the sheet, which results in slower expansion of the sheet. We see that this results in a higher $HT^2$. We note that the left-to-right movement also exists in figure 10 where we changed the Weber number from 100, 200 and 500 but left the same $W$. This phenomenon occurs because the increase in Weber number tells us that there is more kinetic energy transfer, and thus the sheet stretches further, resulting in a lower value of $HT^2$. These lower values result in a shift of the fit from right to left that we observe in figure 10.

## 4.2 Expansion curves

From the nine simulations, we extract the radius and the time to get the expansion curves. The x-axis is the capillary time and on the y-axis is the non-dimensionalized radius times $\sqrt{We_d}$, we use this to get a normalization of the expansion curve. We observe for the same Weber number and an increase in $W$ that the apex of the sheet moves downward on the y-axis as seen in figures 11, 12 and 13. The downward trend occurs because the W parameter increases and so the width of the raised cosine increases. The wider pulse results in a lower maximum radius of the sheet, and so the downward trend is observed. In figure 14 where the $W$ parameter stays the same and $We$ is changed, we note that the apex of the sheet is roughly the same for each Weber number. The increase in Weber number results in a longer radius of the sheet, because a higher Weber number tells us that the inertia is higher and so the sheet thins and spread out more. We scale the curve with the deformation Weber number and then the curves collapse to the same apex time. We also observe three models in the figures 11, 12, 13, 14, a red one with the parameters $b_0 = 0.14, b_2 = -0.58, b_3 = 0.43$ this corresponds to a tin droplet being hit by a laser found by M. Kharbedia et al. [2], a green curve with the parameters $b_0 = 0.12, b_2 = -0.41, b_3 = 0.16$ this corresponds to a water droplet falling onto a pillar found by Y. Wang & L. Bourouiba [3] and a blue curve with the parameters $b_0 = 0.06, b2 = -0.36, b_3 = 0.15$ found by doing an empirical fit of the thickness profile from Liu et al. [7] done by M. Kharbedia et al. [2]. We note that the time of the apex of the models in red, green and blue differ by 0.2 to 0.3 $T/t_c$. This difference, which is larger than experimental values, is in agreement with the expansion curves from the paper of M. Morbey [8]. Who also found a larger apex time of about $0.6T/t_c$. This difference in the apexes could be the case of no mass ejection by the rim. In experiments, the rim ejects mass by decelerating and becomes unstable. This results in small ligaments forming when surface tension takes over these ligaments form into spheres and release from the rim. This could be related to shorter apex times and apex radius in experiments. For the cases of $We = 200$, seen in figures 12a, 12b, 12c and the cases of $We = 500, W = 1.5$, $We = 500, W = 1.75$, seen in figures 13a, 13b, we observe that the apex of the sheet is not part of the data set. The apex is guessed by the curves in the figures 14a, 14b, that hit an apex. This is done because of the collapse of the curves, where all curves of the same $W$ hit the apex at the same time and radius.

### 4.3 Identity

From the identity in equation 11 we can predict the thickness profile from the expansion curve and vise versa. Using the equations 11 to 14 we can find the parameters $b_0, b_2$ and $b_3$, (model 10) from $a_1, a_2$ and $a_3$, (model 8). We fill in the parameters $b_0, b_2, b_3$ to get the parameters $a_1, a_2, a_3$. We note that none of the parameters from the expansion curve result in the thickness profile as seen in figures 15, 16, 17. In these figures the two thickness profiles are plotted, one with the coefficients found by the fit of the simulation and with the coefficients found by the identity by putting in the coefficients of the expansion curve. The two curves do not match, this could be the case because of the late apex time of the expansion sheet. This phenomenon occurs because of the mass that stays in the rim during the evolution of the simulated sheet. However, we checked the findings in the paper of M. Kharbedia et al. [2] and note that the thickness profile parameters correspond to the findings of mathematica for the parameters of the expansion profile and vice versa.

### 4.4 Limitations

One of the limitations found in this research is the refinement of the mesh. The sheet started to break up and have mesh refinement issues at the bottom of the sheet at early times as seen in figure 4. This results in a simulation that is cut short because of that. We can also see that in the expansion curves as seen in figures 14a, 14b. In the cases of $We = 200, W = 1.75$ and $We = 500, W = 1.75$ the apex of the sheet is not hit, so we made assumptions about the location of the apex by means of the apex of the case $We = 100, W = 1.75$. We did the same for the cases with $We = 500, W = 1.5$ and $We = 200, W = 1.5$. Another limitation is that in the simulation the sheet does not shed mass, this results in a larger rim than observed in experiments and a later apex time, this later apex time can be explained by the inertia that stays the same with no mass shed. If mass sheds the momentum of the expansion is transferred to the ligaments and so the sheet retracts earlier. One more limitation is the dimension of the simulation, we simulate in 2D, if we improve the simulation to 3D we can simulate the mass shed in the form of ligaments. We need three dimensions, because the rim is not fully simulated in 2D and no ligaments can form.

## 5 Conclusion

### 5.1 Summary

By performing nine simulations with $We = 100, We = 200, We = 500$ with $W = 1.5, W = 1.75, W = 2$. We compared the simulations with the work of M. Kharbedia [2]. Where we found that the thickness profile fit moved from right to left on the $R/T$ axis with an increase in the $W$ parameter and the $We$ parameter. The parameters of the simulated thickness profile were also different from the experimental thickness profile parameters found in the papers of M. Kharbedia [2] and Y. Wang & L. Bourouiba [3]. We observed that the apex of the expansion sheet moved downward with an increase in $W$. The apex remained roughly the same with a difference in $We$. The time in takes to hit the apex is also longer than observed in the models. This happens because there is no mass shed in the simulation that does occur in experimental setups. Lastly, we looked at the identity found in the paper of Y. Wang & L. Bourouiba [3] where the parameters did not match for the nine simulations but did for the parameters of the experiment carried out by M. Kharbedia et al. [2] and the simulations carried out by Y. Wang & L. Bourouiba [3]. This mismatch can be explained as a result of no mass shed from the rim, which results in a later apex time.

### 5.2 Further recommendation

For future studies on this topic, the mesh refinement should be increased to avoid mesh issues at the bottom of the sheet as seen in figure 4. By solving this issue the simulation can be ran for a longer duration without mesh issues forming and stopping the simulation. Another recommendation is adding mass shed to the simulation to simulate ligaments shed of the sheet, this could improve the apex time of the expansion curve. This can be done by doing simulations in 3D, instead of a 2D simulation. For mass shed we need to go to a 3 dimensional simulation because ligaments form from the rim of the sheet. In our simulations, we have a side view with the thickness and the radial expansion, but not the full rim. So we cannot simulate where on the rim a ligament can form. A wider range of Weber numbers could increase the accuracy of the comparisons with real experiments.

## 6 Acknowledgements

I want to thank Oscar Versolato for letting me work on this project, it was a tough but fun experience. I also want to thank Hugo Franca and Mikheil Kharbedia for guiding me through this project, they always stood ready to answer questions and help me with this project. Lastly, I want to thank the institutes, where I was doing my project, ARCNL and AMOLF, the work environment was welcoming and the personnel where nothing less, many thanks to all!

## References

[1] I. J. Twombly, How it works float-type carburetor, https://www.aopa.org/news-and-media/all-news/2012/april/flight-training-magazine/how-it-works (2012).

[2] M. Kharbedia, *et al.*, Rim destabilization and re-formation upon severance from its expanding sheet, *Submitted* (2025).

[3] Y. Wang, L. Bourouiba, Non-galilean taylor–culick law governs sheet dynamics in unsteady fragmentation, *Journal of Fluid Mechanics* **969** (2023).

[4] H. Franca, H. Karl, Schubert, O. Versolato, M. Jalaal, Laser-induced droplet deformation: curvature inversion explained from instantaneous pressure impulse, *Arxiv* (2025).

[5] J. A. van Hooft, S. Popinet, A fourth-order accurate adaptive solver for incompressible flow problems, *Journal of Computational Physics* **462**, 111251 (2022).

[6] Popinet, Basilisk, http://basilisk.fr/src/navier-stokes/centered.h#correction (2013-2021). Accessed on 7 - 2, 2024.

[7] B. Liu, D. Kurilovich, H. Gelderblom, O. Versolato, Mass loss from a stretching semitransparent sheet of liquid tin, *Physical Review Applied* **13** (2020).

[8] M. Morbey, Numerical simulations of droplet impact by a laser pulse, *Master Thesis* (2021).

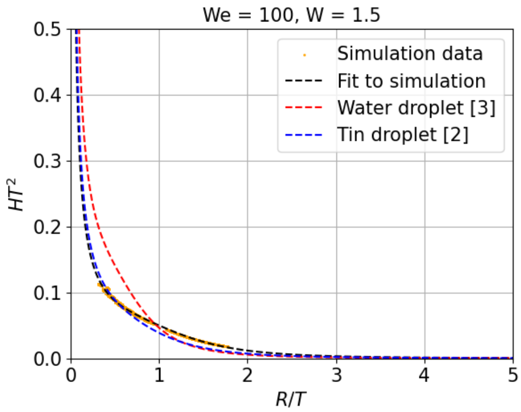


(a) Fit parameters: $a_1 = 35.0, a2 = -33.6, a3 = 18.6$

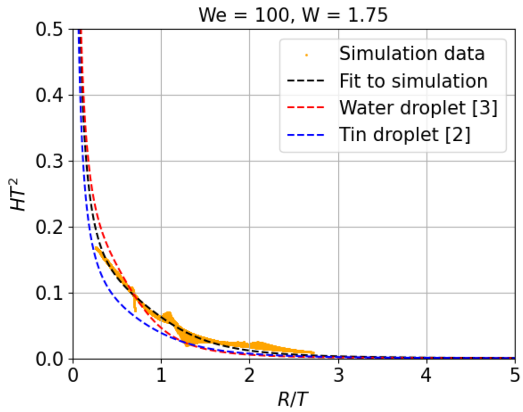


(b) Fit parameters: $a_1 = 25.4, a2 = -27.1, a3 = 17.7$

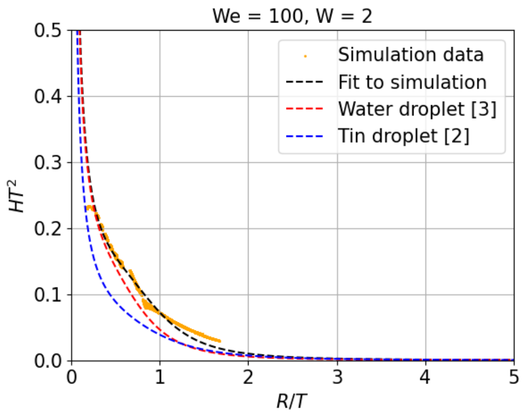


(c) Fit parameters: $a_1 = 23.1, a2 = -32.0, a3 = 22.7$

Figure 7: The non-dimensionalized width plotted against the non-dimensionalized radius for We = 100 and a different W. The orange data points are the data that is obtained from the simulations. These points are then used for a fit where the black dashed line comes from. We also observe a blue and pink line these lines uses the same model with different parameters. The blue line uses the parameters, $a1 = 31.4, a2 = -30.0, a3 = 24.4$, found by M. Kharbedia [2] and for the pink line; $a1 = 24.4, a2 = -28.1, a3 = 35.2$, as found by Y. Wang & L. Bourouiba [3], Comparing these three we observe that the data points shift to right with an increase in W.

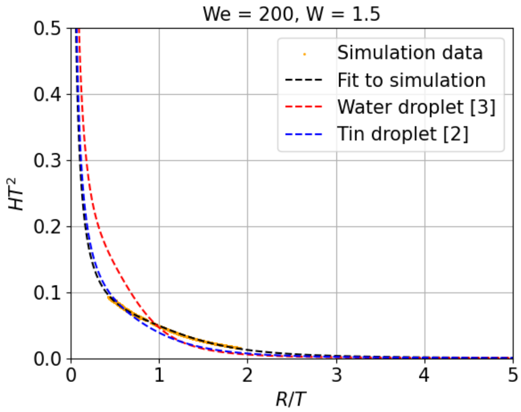


(a) Fit parameters: $a_1 = 34.8, a2 = -31.3, a3 = 16.9$

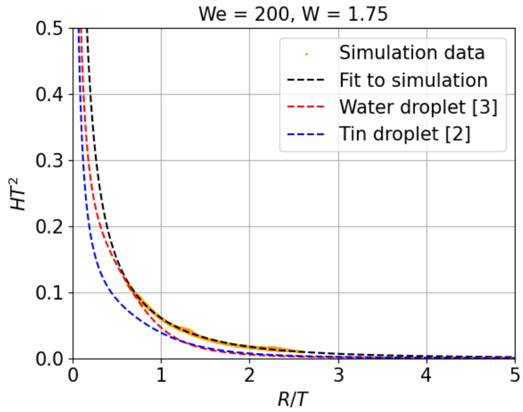


(b) Fit parameters: $a_1 = 12.2, a2 = 0.2, a3 = 4.0$

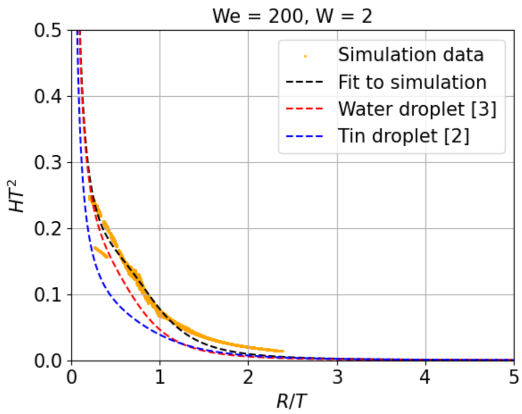


(c) Fit parameters: $a_1 = 23.7, a2 = -36.1, a3 = 25.2$

Figure 8: The non-dimensionalized width plotted against the non-dimensionalized radius for $We = 200$ and a different $W$. The orange data points are the data that is obtained from the simulations. These points are then used for a fit where the black dashed line comes from. We also observe a blue and pink line these lines uses the same model with different parameters. The blue line uses the parameters, $a1 = 31.4, a2 = -30.0, a3 = 24.4$, found by M. Kharbedia [2] and for the pink line; $a1 = 24.4, a2 = -28.1, a3 = 35.2$, as found by Y. Wang & L. Bourouiba [3]. Comparing these three we observe that the data points shift to right with an increase in W.

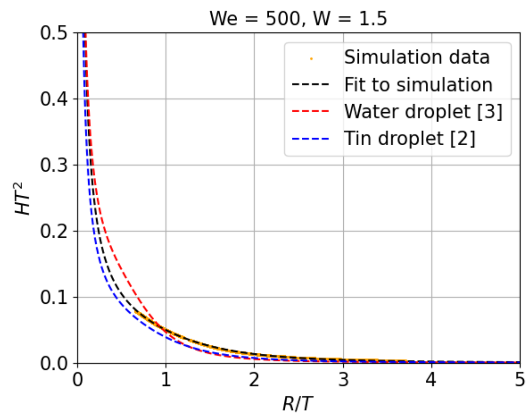


(a) Fit parameters: $a_1 = 23.5, a2 = -13.8, a3 = 10.5$

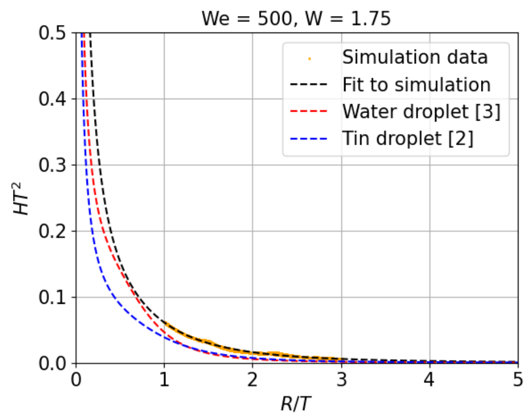


(b) Fit parameters: $a_1 = 12.3, a2 = -1.4, a3 = 5.4$

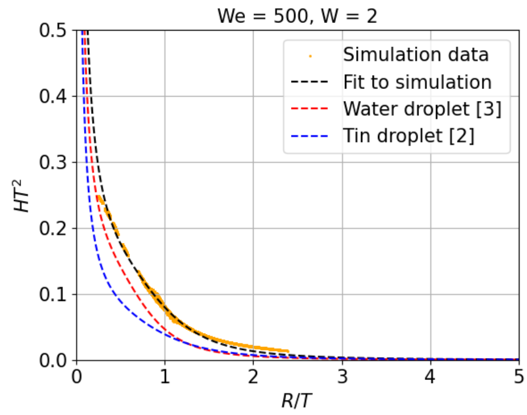


(c) Fit parameters: $a_1 = 17.9, a2 = -20.9, a3 = 15.5$

Figure 9: The non-dimensionalized width plotted against the non-dimensionalized radius for We = 500 and a different W. The orange data points are the data that is obtained from the simulations. These points are then used for a fit where the black dashed line comes from. We also observe a blue and pink line these lines uses the same model with different parameters. The blue line uses the parameters, $a1 = 31.4, a2 = -30.0, a3 = 24.4$, found by M. Kharbedia [2] and for the pink line; $a1 = 24.4, a2 = -28.1, a3 = 35.2$, as found by Y. Wang & L. Bourouiba [3]. Comparing these three we observe that the data points shift to right with an increase in W.

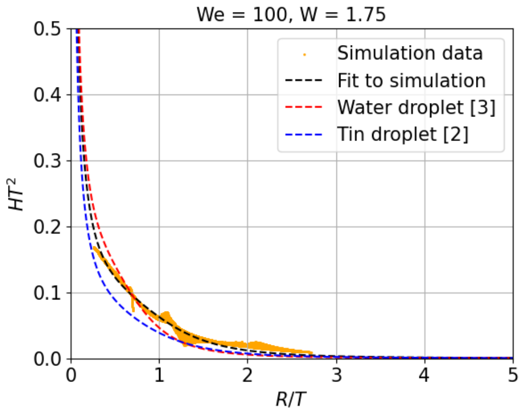


(a) Fit parameters: $a_1 = 25.4, a2 = -27.1, a3 = 17.7$

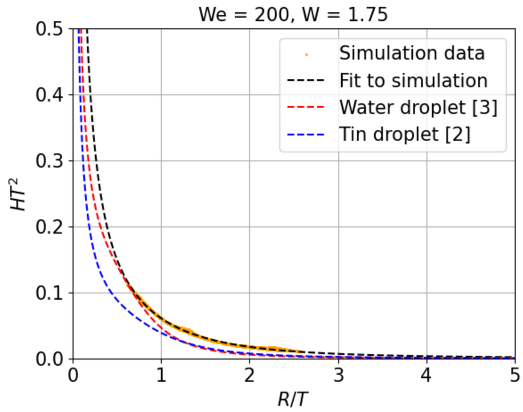


(b) Fit parameters: $a_1 = 12.2, a2 = 0.2, a3 = 4.0$

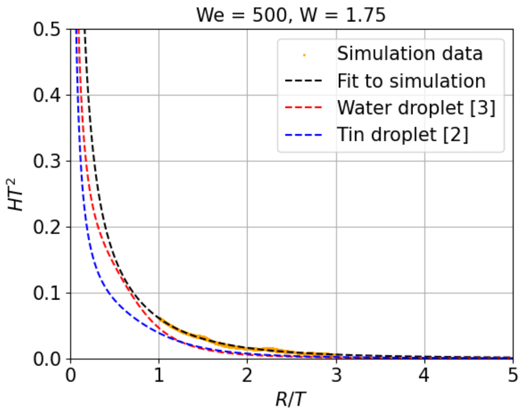


(c) Fit parameters: $a_1 = 12.3, a2 = -1.4, a3 = 5.4$

Figure 10: In these three graphs is the non-dimensionalized width plotted against the non-dimensionalized radius for different Weber number and the same W. With the orange points the data from the simulations. The black line is the fit achieved by using the orange points. We also observe a blue and pink line these lines uses the same model with different parameters. The blue line uses the parameters, $a1 = 31.4, a2 = -30.0, a3 = 24.4$, found by M. Kharbedia [2] and for the pink line; $a1 = 24.4, a2 = -28.1, a3 = 35.2$, as found by Y. Wang & L. Bourouiba [3]. Comparing the three plots we observe that the black line has a shift from left to right in the R / T - axis with an increase in Weber number.

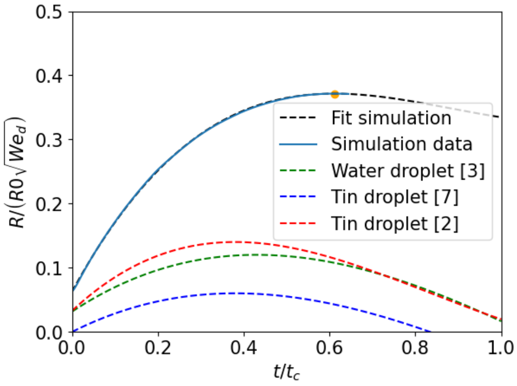


(a) $We = 100, W = 1.5$

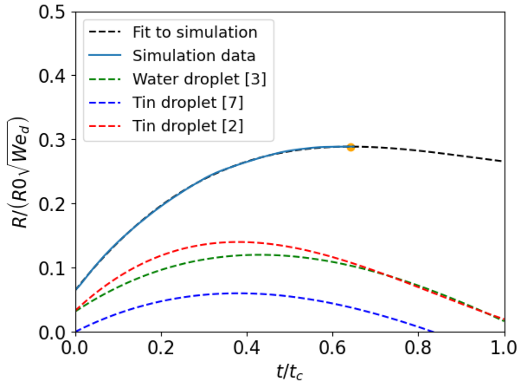


(b) $We = 100, W = 1.75$

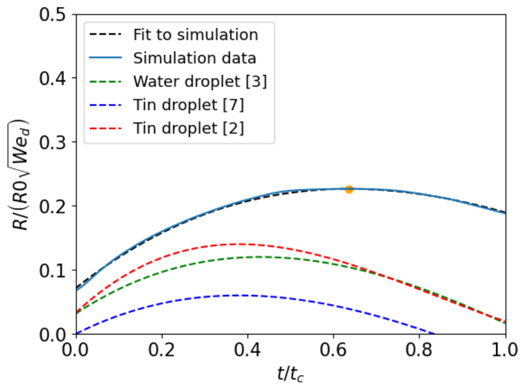


(c) $We = 100, W = 2$

Figure 11: We plot the non-dimensionalized radius against the capillary time this is done for $We = 100$. The blue line is the data with the orange point being the apex of the expansion sheet. Where we fit on getting the black dashed line with the parameters in a) $b_0 = 0.37, b_2 = -0.47, b_3 = 0.58$, in b) $b_0 = 0.29, b_2 = -0.31, b_3 = 0.36$ and in c) $b_0 = 0.23, b_2 = -0.32, b_3 = 0.11$. We also observe a red, ($b_0 = 0.14, b_2 = -0.58, b_3 = 0.43$) [2], blue ($b_0 = 0.06, b_2 = -0.36, b_3 = 0.15$) [7], and green ($b_0 = 0.12, b_2 = -0.41, b_3 = 0.16$) line [3], which are models used in the paper of M. Kharbedia [2]. If looked at the apex of the curve we observe a decrease of the apex with an increase in $W$, where $We$ stays the same.

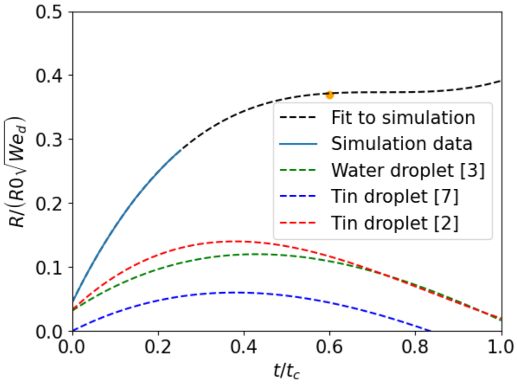


(a) $We = 200, W = 1.5$

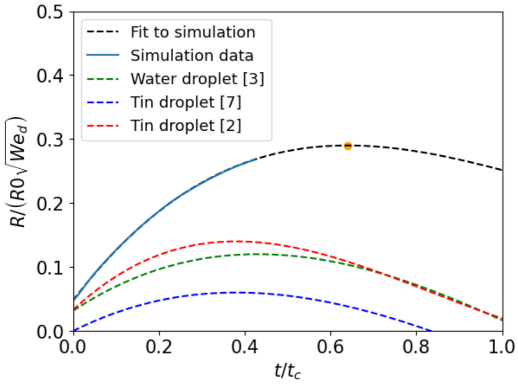


(b) $We = 200, W = 1.75$

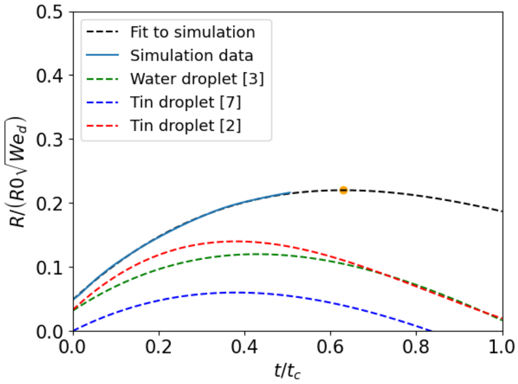


(c) $We = 200, W = 2$

Figure 12: We plot the non-dimensionalized radius against the capillary time, this is done for $We = 200$. The blue line is the data with the orange point being the apex of the expansion sheet. Where we fit on getting the black dashed line with the parameters in a) $b_0 = 0.37, b_2 = -0.0, b_3 = 0.86$, in b) $b_0 = 0.29, b_2 = -0.4, b_3 = 0.29$ and in c) $b_0 = 0.22, b_2 = -0.31, b_3 = 0.19$. We also observe a red, ($b_0 = 0.14, b_2 = -0.58, b_3 = 0.43$) [2], blue ($b_0 = 0.06, b_2 = -0.36, b_3 = 0.15$) [7], and green ($b_0 = 0.12, b_2 = -0.41, b_3 = 0.16$) line [3], which are models used in the paper of M. Kharbedia [2]. If looked at the apex of the curve we observe a decrease of the apex with an increase in $W$, where $We$ stays the same.

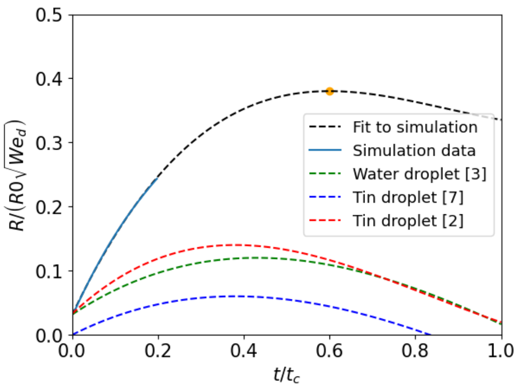


(a) $We = 500, W = 1.5$

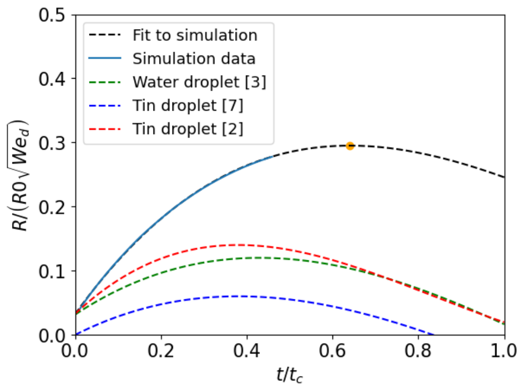


(b) $We = 500, W = 1.75$

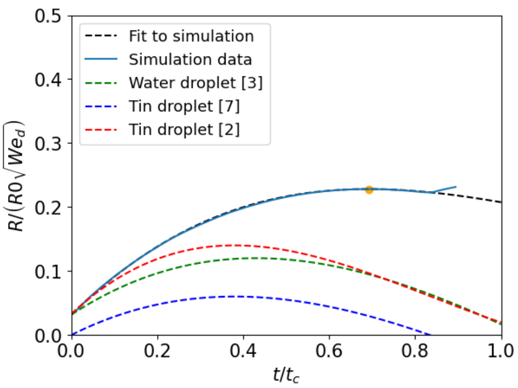


(c) $We = 500, W = 2$

Figure 13: We plot the non-dimensionalized radius against the capillary time, this is done for $We = 500$. The blue line is the data with the orange point being the apex of the expansion sheet. Where we fit on getting the black dashed line with the parameters in a) $b_0 = 0.38, b_2 = -0.56, b_3 = 0.69$, in b) $b_0 = 0.29, b_2 = -0.47, b_3 = 0.26$ and in c) $b_0 = 0.23, b_2 = -0.28, b_3 = 0.2$. We also observe a red, ($b_0 = 0.14, b_2 = -0.58, b_3 = 0.43$) [2], blue ($b_0 = 0.06, b_2 = -0.36, b_3 = 0.15$) [7], and green ($b_0 = 0.12, b_2 = -0.41, b_3 = 0.16$) line [3], which are models used in the paper of M. Kharbedia [2]. If looked at the apex of the curve we observe a decrease of the apex with an increase in $W$, where $We$ stays the same.

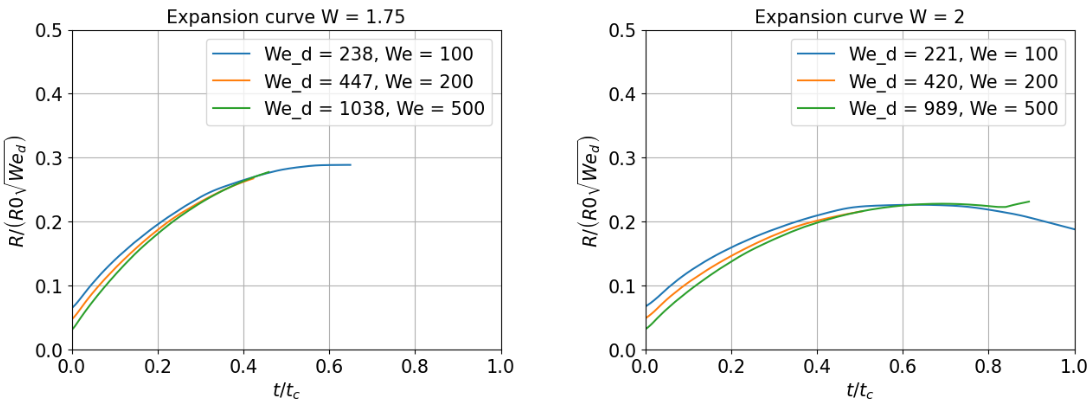


(a)

(b)

Figure 14: We plot the non-dimensionalized radius against the capillary time. We plot $W = 1.75$ for figure 14a and $W = 2$ for figure 14b. For each of the plots we plot the different We numbers. The blue curve is $We = 100$, the orange curve is $We = 200$ and the green curve is $We = 500$.

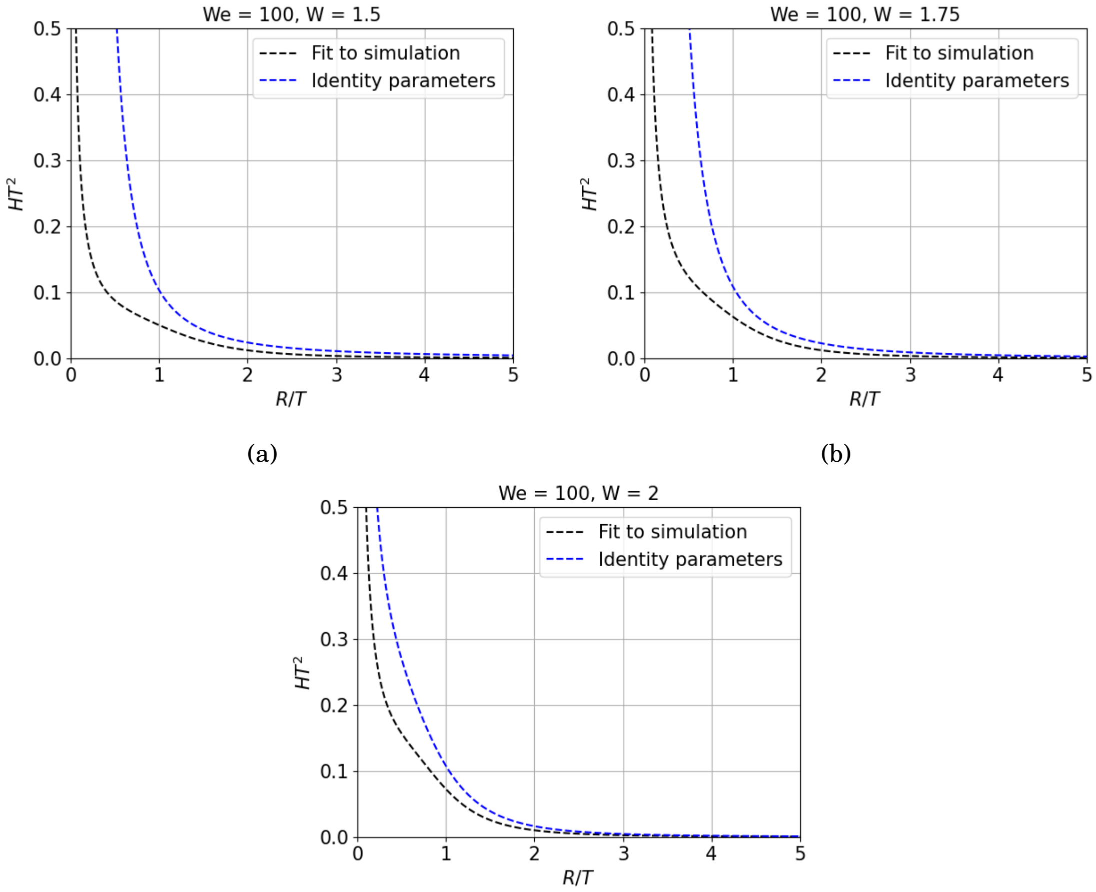

(a) (b) (c)

Figure 15: The non-dimesnional width is plotted against the non-dimensional radius. We see a black curve and a blue curve, the black curve is the thickness profile fit and the blue is the thickness profile found by using the identity. In panel a) the coefficients are, blue: $a_1 = -2.9, a_2 = 13.2, a_3 = -0.6$ and black: $a_1 = 35.0, a_2 = -33.6, a_3 = 18.6$. In panel b) the coefficients are, blue: $a_1 = -0.8, a_2 = 8.5, a_3 = 1.5$ and black: $a_1 = 25.4, a_2 = -27.1, a_3 = 17.7$. In panel c) the coefficients are, blue: $a_1 = 11.5, a_2 = -14.12, a_3 = 11.9$ and black: $a_1 = 23.09, a_2 = -32.0, a_3 = 22.7$

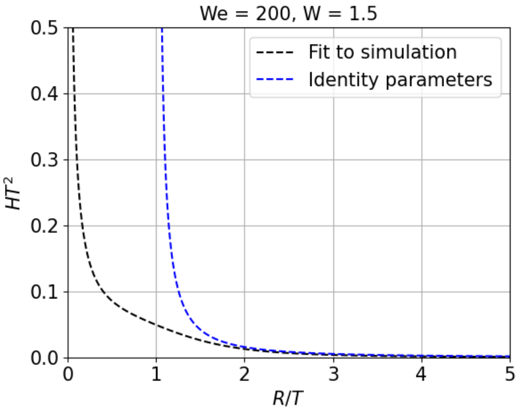


(a)

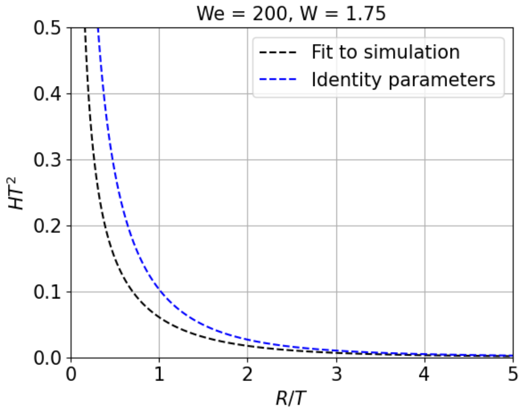


(b)

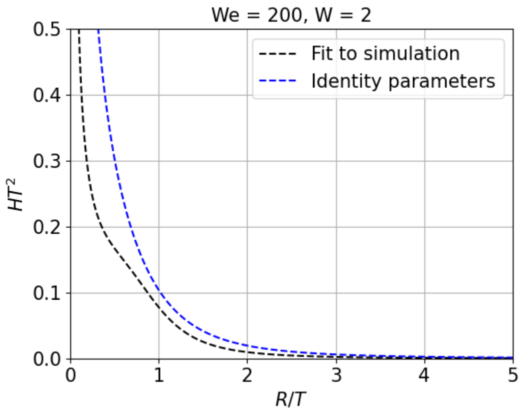


(c)

Figure 16: The non-dimesnional width is plotted against the non-dimensional radius. We see a black curve and a blue curve, the black curve is the thickness profile fit and the blue is the thickness profile found by using the identity. In panel a) the coefficients are, blue: $a_1 = -32.7, a_2 = 32.5, a_3 = -0.1$ and black: $a_1 = 34.8, a_2 = -31.3, a_3 = 16.9$. In panel b) the coefficients are, blue: $a_1 = 5.8, a_2 = 1.4, a_3 = 2.5$ and black: $a_1 = 12.2, a_2 = 0.2, a_3 = 4$. In panel c) the coefficients are, blue: $a_1 = 6.9, a_2 = -4.0, a_3 = 6.7$ and black: $a_1 = 23.7, a_2 = -36.1, a_3 = 25.2$.

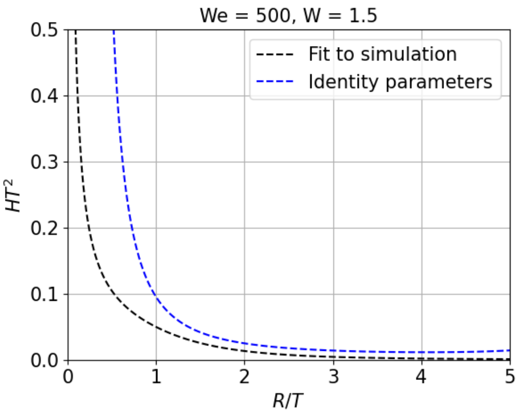


(a)

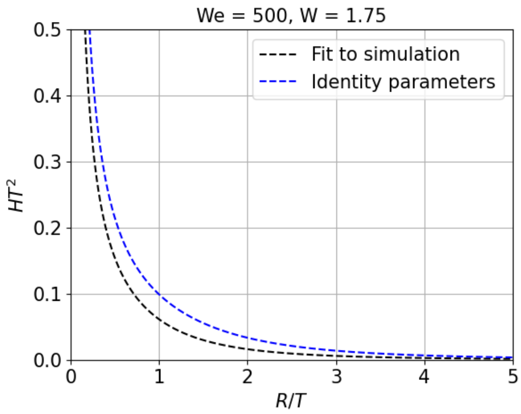


(b)

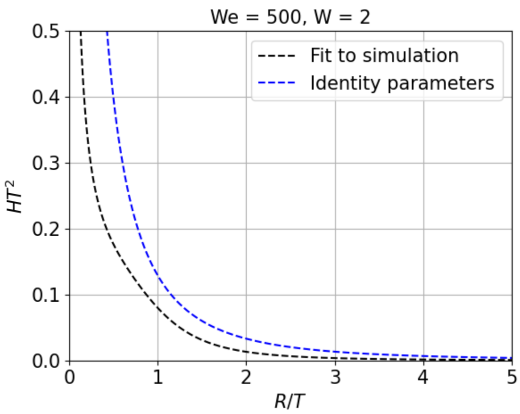


(c)

Figure 17: The non-dimesnional width is plotted against the non-dimensional radius. We see a black curve and a blue curve, the black curve is the thickness profile fit and the blue is the thickness profile found by using the identity. In panel a) the coefficients are, blue: $a_1 = -4.9, a_2 = 18.3, a_3 = -2.9$ and black: $a_1 = 23.5, a_2 = -13.8, a_3 = 10.5$. In panel b) the coefficients are, blue: $a_1 = 9.6, a_2 = -1.7, a_3 = 2.2$ and black: $a_1 = 12.3, a_2 = -1.4, a_3 = 5.4$. In panel c) the coefficients are, blue: $a_1 = 3.0, a_2 = 3.5, a_3 = 1.3$ and black: $a_1 = 17.9, a_2 = -20.9, a_3 = 15.5$.